ELSEVIER

Physica A 207 (1994) 197–207

PHYSICA A

Fractals: Localization of dipole excitations and giant optical polarizabilities

Vladimir M. Shalaev[a,1] R. Botet[b], D.P. Tsai[c], J. Kovacs[c], Martin Moskovits[c]

[a]*Department of Physics, New Mexico State University, Las Cruces, NM 88003, USA*
[b]*Laboratoire de Physique des Solides, Université Paris-Sud, Centre d'Orsay, 91405 Orsay Cedex, France*
[c]*Ontario Laser and Lightwave Research Centre, and Department of Chemistry, University of Toronto, Toronto, Ontario M5S 1A1, Canada*

Abstract

Highly localized optical modes laser-excited on silver colloid fractal clusters were observed using photon scanning tunnelling microscopy (PSTM). The spatial distribution of the modes excited shows the frequency and polarization selectivity suggested by numerical simulations. The localization of the optical excitations on fractals results in very high local fields leading to the huge enhancement of resonant Rayleigh, Raman and, especially, nonlinear light scattering. The experimental results verify the main concepts of the developed resonant optical theory of fractals.

The localization of dynamical excitations in disordered systems and, specifically, in fractals is of interest because of its universality and its role in many physical processes [1–5]. In particular, localization of dipole eigenmodes can lead to a dramatic enhancement of many optical effects in fractals [6]. The scaling theory of collective dipole excitations developed in [7–9] predicts that the dipolar eigenmodes of fractal clusters are localized in regions smaller than the wavelength [7,9] and can, therefore, concentrate electrical energy in areas smaller than the diffraction limit of conventional optics. It is this localization of optical excitations in fractal clusters that account for the very high local fields leading to the huge enhancement of resonant Rayleigh, Raman and, especially, of nonlinear light scattering [10,11]. In addition to the localization of light-induced dipole excitations fractality can result in the localization (trapping) of the light itself within a range of the order of a wavelength [12]. An important property of the interaction

[1] Author to whom correspondence should be addressed.

Elsevier Science B.V.
SSDI 0378-4371(93)E0536-N

of light with fractals is the very strong frequency and polarization dependence of the spatial location of the light-induced dipole modes. In this paper we present numerical simulations and direct experimental observations of localized optical modes on silver colloid fractal clusters.

The number of particles, N, forming a fractal aggregate is given by $N=(R_c/R_0)^D$ where R_c is the radius of gyration of the cluster and R_0 is a typical separation between neighbour monomers. Light-induced dipole–dipole interaction between the polarizable particles in the aggregate is determined by the complex polarizability χ_0 of an isolated monomer. Defining $Z\equiv\chi_0^{-1}$, $X\equiv-\mathrm{Re}\,Z$, and $\delta\equiv-\mathrm{Im}\,Z$, X plays the role of a spectral variable and δ expresses the dielectric losses. If the monomers are spherical particles with $\chi_0=R_m^3(\epsilon-1)/(\epsilon+2)$, then $X=-R_m^{-3}(|2\epsilon+1|^2-9)/(4|\epsilon-1|^2)$, and $\delta=3R_m^{-3}\epsilon''/|\epsilon-1|^2$ where $\epsilon=\epsilon'+i\epsilon''$ is the dielectric constant of the material of which the particle is comprised. In the vicinity of the localized surface plasmon (LSP) resonance with frequency ω_0 (defined by $\epsilon'(\omega_0)=-2$), $X\propto\omega-\omega_0$ where ω is the frequency of light. $Q=(R_0^3\delta)^{-1}$ defines the quality factor of the resonance. Q for the LSP resonance induced on a fractal aggregate of spherical particles is given by $Q=(R_m/R_0)^3|\epsilon-1|^2/3\epsilon''$ [6,7,9]. For Ag at 500 nm Q is $\sim10^2$ [10].

An external electrical field, whose value at the site of the ith monomer ($i=1,2,\ldots,N$) is equal to $\tilde{E}_\alpha^i=E_\alpha^{(0)}\exp(-i\omega t+i\boldsymbol{k}\cdot\boldsymbol{r}_i)$, induces the transitional dipole moment $\tilde{d}_\alpha^i=d_\alpha^i\exp(-i\omega t+i\boldsymbol{k}\cdot\boldsymbol{r}_i)$ ($\alpha=x,y,z$). We introduce the $3N$-dimensional vectors $|d)$ and $|E^{(0)})$ with components $(i\alpha|d)=d_{i\alpha}$ and $(i\alpha|E^{(0)})=E_\alpha^{(0)}$. Similar notations will be also used for other vectors. The equation for $|d)$ acquires the form

$$Z|d)=|E^{(0)})-V|d)\,, \tag{1}$$

where

$$(i\alpha|V|j\beta)=\frac{a^{ij}\delta_{\alpha\beta}-3b^{ij}n_\alpha^{(ij)}n_\beta^{(ij)}}{r_{ij}^3}\exp(ikr_{ij}-i\boldsymbol{k}\cdot\boldsymbol{r}_{ij})\,, \tag{2}$$

$$a^{ij}=1-ikr_{ij}-(kr_{ij})^2\,,\qquad b^{ij}=1-ikr_{ij}-\tfrac{1}{3}(kr_{ij})^2\,.$$

Here V is the dipole–dipole interaction operator ($V=0$ for $i=j$), $\boldsymbol{r}_{ij}=\boldsymbol{r}_i-\boldsymbol{r}_j$ and $\boldsymbol{n}^{ij}=\boldsymbol{r}_{ij}/r_{ij}$. The interaction (2) includes the near-zone (nonradiative), transitional and far-zone (radiative) terms of the dipole field.

It was shown in [10] that if $R_0^3|X|\gg(R_0/\lambda)^{3-D}$ for $D<2$ and if $R_0^3|X|\gg(R_0/\lambda)N^{1-2/D}$ for $D>2$, then particles positioned at distances $r_{ij}\sim\lambda$ and $r_{ij}\gg\lambda$ from a given monomer, i, contribute negligibly to the local field acting on this monomer. In this case one can reduce V in (1), (2) to the Hermitian near-zone dipole–dipole interaction operator [10]

$$(i\alpha|W|j\beta)=\begin{cases}(\delta_{\alpha\beta}-3n_\alpha^{(ij)}n_\beta^{(ij)})r_{ij}^{-3}\,, & \text{if } kr_{ij}<1\,,\quad i\neq j\,,\\ 0\,, & \text{otherwise}\,.\end{cases} \tag{3}$$

Introducing eigenvectors $|n)$ and the corresponding eigenvalues w_n of the W operator, one finds that the polarizability of the $i$the monomer [7] has the form [12]

$$\chi^{(i)}_{\alpha\beta} = \sum_n a^{(i)}_{n,\alpha}\chi^{(c)}_{n,\beta}\,,$$
$$a^{(i)}_{n\alpha} = (i\alpha|n)\,, \qquad \chi^{(c)}_{n,\alpha} = \sum_i a^{(i)}_{n,\alpha}(\chi_0^{-1} + w_n)^{-1}\,. \tag{4}$$

Thus, strong dipole interaction leads to a renormalization of the problem from one of the N dipoles in a cluster to one of $3N$ collective dipolar eigenmodes with polarizabilities $\chi^{(c)}_{n,\alpha}$ ($(n|d) \equiv d_n = \chi^{(c)}_{n,\alpha}E^{(0)}_\alpha$) which contribute to the polarizability of the ith monomer with weight $a^{(i)}_{n,\alpha}$. It is shown in [7,9] that dipole eigenmodes are localized on fractals within correlation length L_X given by

$$L_X \sim R_0(R_0^3|X|)^{(d_o-1)/(3-D)} \tag{5}$$

where d_o is an index called the optical spectral dimension ($0 < d_o < 1$) [7]. Formula (5) was obtained by assuming that collective excitations of large coherence length L_X are invariant with respect to the scale transformation $R_0 \to R_0'$ due to self-similarity [7]. These scaling arguments are valid only when $R_0 \ll L_X \ll R_c,\ \lambda$.

Note, that the localization of dipole excitation on fractals is a nontrivial fact. Since the dipole–dipole interaction for compact aggregates ($D \to 3$) is long range, dipole modes are generally delocalized over the entire cluster.

In Fig. 1 three different dipole eigenmodes of the fractal are presented. Each mode is determined by certain value of the dimensionless spectral variable $R_0^3|X|$ ($R_0 \equiv 1$). The cluster was simulated by the cluster-cluster aggregation [13]. Points in the figure correspond to the centres of particles touching each other and forming the cluster. Radii of the circles drawn around the particles give the value of dipole moments induced on them. These dipole moments were calculated by

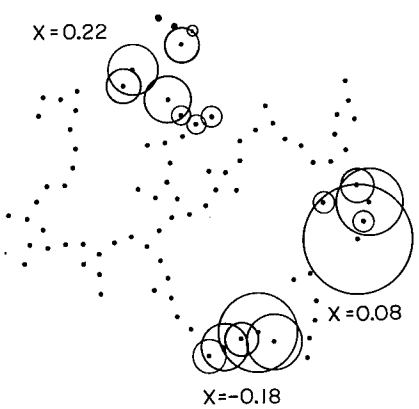

Fig. 1. Localized dipole modes on the fractal.

determining the eigenvectors and eigenvalues of the interaction operator W in (3) and substituting them to Eqs. (4). It is clear from the figure that strong localization of the collective dipole modes occurs for the fractal.

Below we present numerical simulations and direct experimental observations of local fields due to excitation of the localized dipole modes on silver colloid fractal clusters by means of photon scanning tunneling microscopy (PSTM). By operating in the near-zone of the dipole fields PSTM can overcome the traditional diffraction limit thereby imaging details smaller than the wavelength [14]. Optical excitations of fractal aggregates can be observed with PSTM by placing the clusters in the evanescent (external) field of a laser beam totally internally reflected in a glass prism.

We will make the simplifying assumption that the signal detected by the tapered optical fiber tip of the PSTM is proportional to the squared modulus of the local field which is the sum of the evanescent field of amplitude $E_\alpha^{(0)}$ and the fields of the dipoles with amplitudes $d_\alpha^{(i)} = \chi_{\alpha\beta}^{(i)} E_\beta^{(0)}$ induced in the particles forming the cluster. The intensity is given by

$$I = \left| E_\alpha^{(0)} \mathrm{e}^{-\alpha z} - \sum_j V_{\alpha\beta}^{(ij)} \chi_{\beta\gamma}^{(j)} E_\gamma^{(0)} \, \mathrm{e}^{-\alpha z_j} \right|^2 . \tag{6}$$

The inverse decay length of the evanescent field along the normal to the surface, z, is $\alpha = (2\pi/\lambda)(n^2 \sin^2 \Theta - 1)^{1/2}$. Here λ is the vacuum wavelength of the light, n is the refractive index of the prism, and Θ is the incident angle.

The results of our numerical simulation of the intensity distribution, $I(x, y, z = z_0)$, of local fields due to the excitation of dipole eigenmodes on fractal aggregates are shown in Fig. 2. A three-dimensional cluster with $N = 512$ was generated assuming cluster–cluster aggregation [13] ($D \approx 1.78$). The 3D cluster was collapsed to its two-dimensional projection simulating closely the experimental situation. The dipole excitations and local fields values were calculated using equations (3), (4), (6), and assuming the following parameter values: $\delta = 0.01$ ($R_0 \equiv 1$), $z_0/R_\mathrm{m} = 2$ where R_m is the radius of particles and $\lambda/R_\mathrm{m} = 50$. (This corresponds to the experimental situation where $R_\mathrm{m} \simeq 10$ nm and $\lambda \simeq 500$ nm.) The figure shows $I(x, y)$ at two values of the light frequency and for both, s and p, polarizations. Note that the intensity of local fields strongly fluctuates and it is significantly larger than the external field in spatially localized regions of the cluster. The localization of the high-field regions reflects the localization of the dipole eigenmodes presented in Fig. 1. It also follows from Fig. 2 that several quasiresonant eigenmodes can be excited simultaneously by the external field. The linear dimension of the high-local-field regions in Fig. 2 varies from mode to mode. On average a mode spans several hundred Å when $R_\mathrm{m} = 100$ Å. The frequency and polarization sensitivity of the mode localization is evident in Fig. 2: a change of either light frequency (parameter X) or polarization results in the excitation of new resonant modes with different spatial locations and intensities.

Fractal clusters resulting from cluster–cluster aggregation of colloid particles

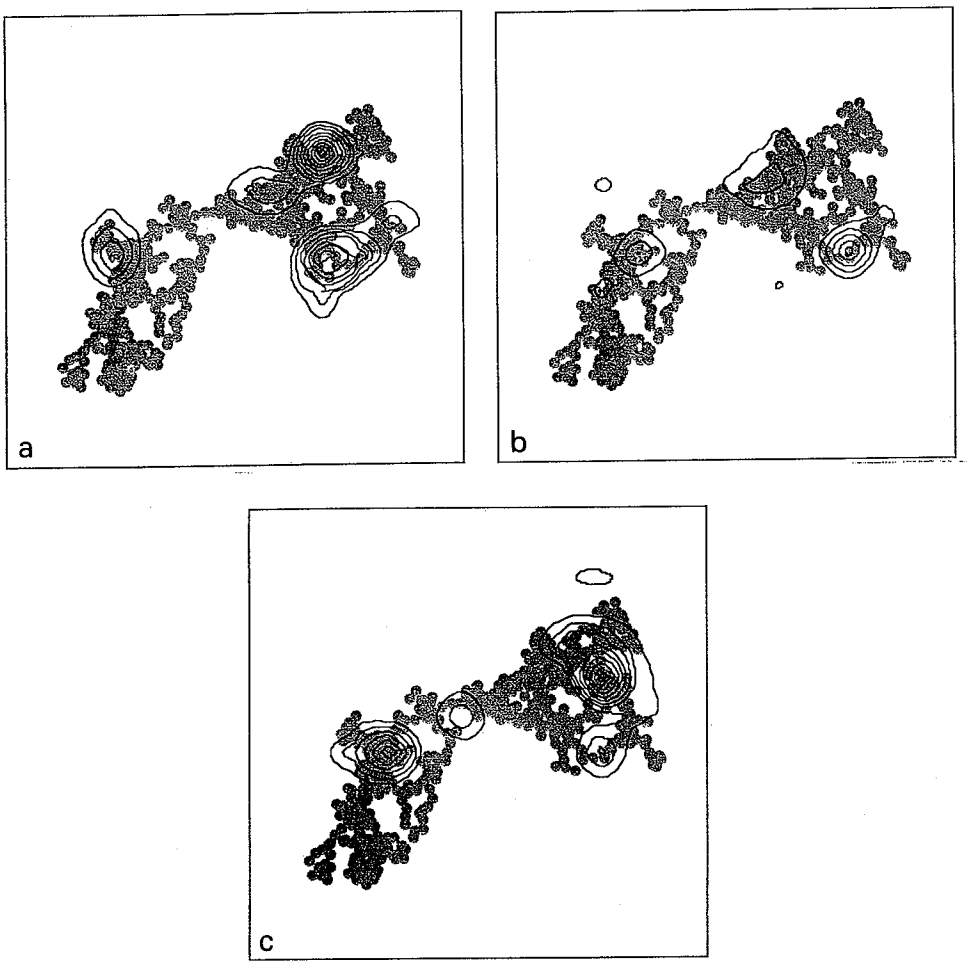

Fig. 2. Local field intensity, $I(x, y)$, of the light-induced dipole modes calculated for a fractal aggregate. (a), (b) $X = -0.1$, s- and p-polarizations, respectively; (c) $X = -0.25$, s-polarization.

are random. Their scale-invariance is statistical. Spatial localization of light-induced dipole modes and their sensitivity to polarization and frequency should also be observed on geometrically ordered fractals. Fig. 3 shows $I(x,y)$ for a Vicsek cluster, using parameters similar to those used previously to generate Fig. 3 except that $\lambda/R_m = 25$. Again, strong localization of the optical excitations is evident. Interestingly, there is no symmetry in the positions of the light-induced eigenmodes despite the high symmetry of the Viscek fractal. The symmetry breaking results from the incommensurate structure of the light field with respect to that of the cluster. Specifically it is the introduction of the two vectors, $\boldsymbol{E}^{(0)}$ and $\boldsymbol{k}$, together with the tensor character of the dipole–dipole interaction that breaks symmetry.

The experiments were carried as follows. A right-angle BK-7 glass prism was

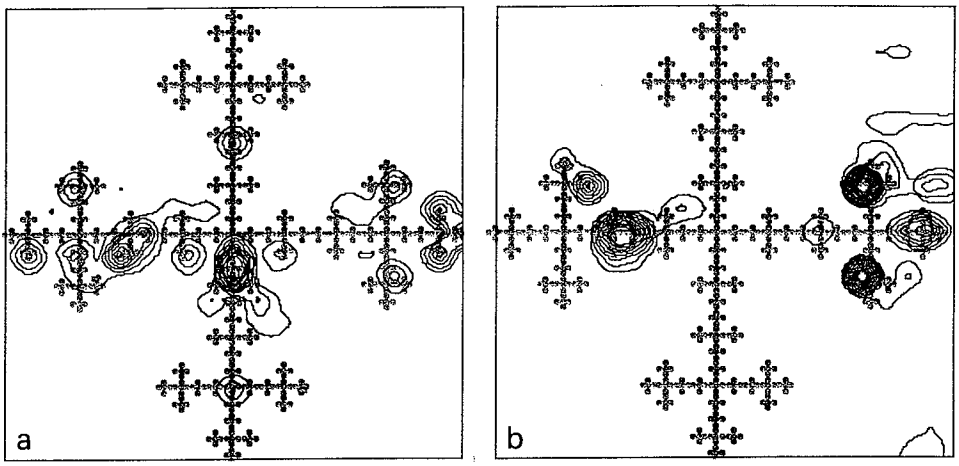

Fig. 3. Local field intensity, $I(x, y)$, of the light-induced dipole modes on a Vicsek fractal. (a), (b) s-polarization, $X = -0.1$ and $X = -0.25$, respectively.

illuminated normal to one of the small faces resulting in total internal reflection at the hypotenuse-face. A tapered optical fiber was mounted in a piezoelectric tube scanner with a maximum scanning area of $9\,\mu m \times 9\,\mu m$ allowing controlled movement of the tip on a nanometer scale in the three canonical directions. The tapered fiber tips were fabricated by pulling a single-mode, graded-index fiber at constant force while locally heating it in the discharge produced by the arc electrodes of a commercial fiber splicer. In order to reduce contamination of the signal by stray light the fibers were gold-coated obliquely in a commercial vacuum coating apparatus, so as to avoid gold deposition at the tip. The effective optical aperture of the tip used in this study is estimated using a technique described in [15] to be in the range from 20 to 50 nm. The light coupled into the fiber was detected by a photomultiplier. The tip height (z) was adjusted piezoelectrically by means of feedback electronics so as to keep the detected light intensity at a constant pre-set value I_s. The piezo z-control voltage was then displayed as a function of x and y to form a three-dimensional image.

Fractal aggregates of silver colloid particles were produced by first generating a silver sol by reducing silver nitrate with sodium boronhydride [16]. Addition of an adsorbate (phthalazine) promotes aggregation, in this case forming fractal colloid cluster having fractal dimension $D \approx 1.78$ [17]. Electron micrograph of a silver colloid cluster resulting from the clister-cluster aggregation is given in Fig. 4. Clusters were allowed to settle slowly out of solution onto microscope cover slides for PSTM imaging. Index matching oil was used to mount the microscope slide to the prism.

Before proceeding further it is instructive to consider how the optical modes will be imaged by the PSTM. The local fields due to the resonant dipole modes are significantly larger than the external evanescent field. The quality factor, Q, characterizes the corresponding enhancement [6,7,10]. Accordingly, for resonant

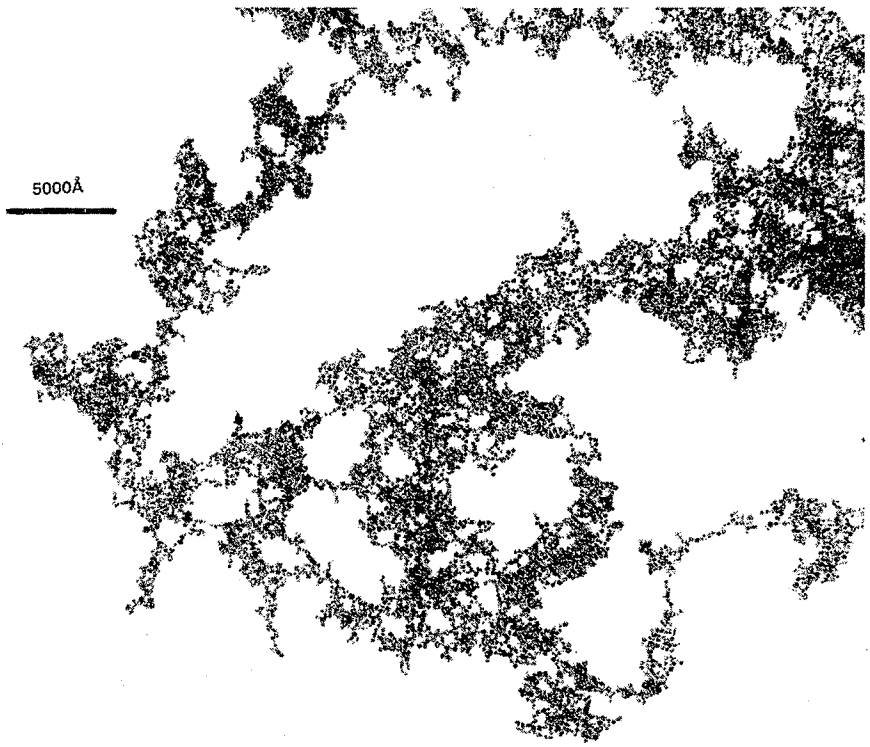

Fig. 4. Electron micrograph of a silver colloid cluster.

eigenmodes the second term in Eq. (6) is of the order of $QE^{(0)}$. Thus, there are three physically different contributions to the detected signal $I(x, y)$ in (6): a background signal $|E^{(0)}e^{-\alpha z}|^2$, the interference part, $\sim[E^{(0)}|^2 Q \exp[ikr_{tj} - i\boldsymbol{k}\cdot\boldsymbol{r}_{tj}]$, and the largest contribution, $\sim|E^{(0)}Q|^2$, due to excitation of resonant fractal modes. The dipole eigenmodes are characterised by a spatial localization dimension, l_X, whose average value determines L_X in (5). The field due to the excitation of a given mode decreases at $r > l_X$ as r^{-3} (r is a distance from the mode centre to the point of observation) so that the corresponding intensity, $I(r)$, decreases as r^{-6}. Thus $I(r) \simeq I_0$ for $r \leq l_X$ and $I(r) \simeq I_0(l_X/r)^6$ for $r > l_X$ where $I_0 \simeq Q^2|E^{(0)}|^2$ is the enhanced intensity within the excited mode. This approximation for $I(r)$ is valid up to $r \sim \lambda$. Let us assume that the tip of PSTM, operating in the constant intensity mode, $I_s \simeq |E^{(0)}|^2$, first scans a "dark" region of the aggregate where there are no excited dipole modes. When approaching the excited mode, the tip will move along a bell-like surface defined by $I(r) = I_s$ and characterized by radius R_X such that $Q^2(l_X/R_X)^6 \simeq 1$. Therefore, the image of an eigenmode with localization length l_X will be magnified by the PSTM so that its characteristic radius is approximately $R_X \simeq Q^{1/3} l_X$. For silver aggregates with $Q \simeq 10^2$, $R_X \simeq 5l_X$. Hence, the PSTM images of excited dipole eigenmodes are expected to be larger than l_X by approximately a factor of 5.

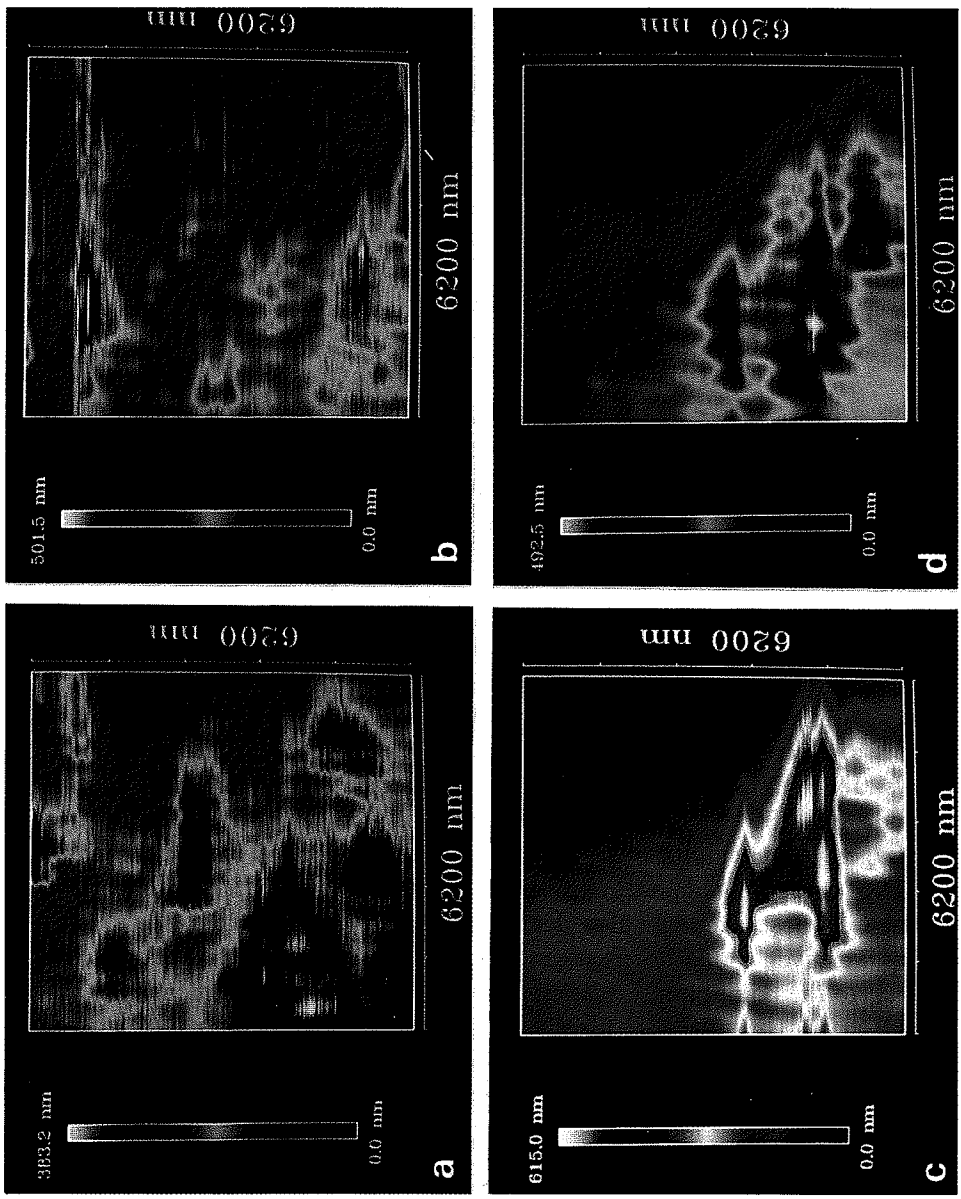

Fig. 5. Photon STM images of local fields in fractal silver colloid aggregates irradiated by light of varying wavelengths and polarizations. (a), (b) $\lambda = 488$ nm, s- and p-polarizations, respectively; (c), (d) p-polarization, $\lambda = 488$ nm and $\lambda = 514.5$ nm, respectively. Two different samples were used to obtain images (a), (b) and images (c), (d).

Photon STM images of silver fractal aggregates are shown in Fig. 5 for different wavelengths and polarizations. The images shown in the figure are similar to those simulated numerically. In particular the images demonstrate the localization of the high-field area corresponding to the dipole eigenmodes as well as the sensitivity of their spatial location to frequency and polarization. The radii of the images of the excited optical eigenmodes, R_X, are measured to range from 300 nm to 700 nm. Accordingly, the localization length, l_X, lies in the range from 60 nm to 140 nm in agreement with the results of the numerical simulations. The interference fringes which arise from the term $\propto \exp[ikr_{tj} - i\boldsymbol{k}\cdot\boldsymbol{r}_{tj}]$ in (6) are also clearly seen. Since for some of the resonant modes in the figure, $2R_X$ is larger than the wavelength one can see the interference fringes within the bright spots.

The colour scale used to indicate the height of the tip above the surface is given on the left side of the images in Fig. 5. We estimate that for the "dark" regions the height of the tip, z_0, is noticeably less than 100 nm. At a resonant dipole mode the tip pulls up to a height $z_{\max} \simeq 400$ to 600 nm. Using the approximate relation $Q^2(l_X/z_{\max})^6 \simeq 1$ and $l_X \simeq 100$ nm, $z_{\max} \simeq 500$ nm one obtains $Q \simeq 125$ in reasonable agreement with values estimated from the optical constants of silver [10]. Hence all aspects of the observed images accord well with those expected on the basis of our calculations.

As it was shown above dipole eigenmodes on fractals "produce" small regions of very high energy density and, therefore, they act in some sense similar to optical lenses. Since the modes on fractals are mostly due to the dipole–dipole interaction in the near-zone the localization length is significantly smaller than the wavelength. Thus the excitation of the resonant modes should lead to extremely high local fields resulting in its turn in giant enhancement of many optical processes on fractals.

Local fields, E_ℓ, of the resonant modes exceed the external one, $E^{(0)}$, by a factor Q. The fraction of monomers involved into resonant excitation is small, $\sim Q^{-1}$, and, therefore, linear optical processes are not ultimately enhanced (note, however, that for metal aggregates this conclusion is restricted to the visible and the near-infrared portion of the spectrum when one can neglect the Ohmic current in comparison with the displacement current). For nonlinear optical process, $\propto |E|^n$, one obtains [6,11]

$$\langle |E_\ell/E^{(0)}|^n \rangle \sim Q^n \times Q^{-1} \sim Q^{n-1} \gg 1\,, \tag{7}$$

where $\langle \ldots \rangle$ indicates averaging over ensemble of clusters. The estimation (7) is valid, in general, for systems with inhomogeneous broadening. Note that for coherent processes on fractals, when the phase relations are of importance, the approximation (7) remains valid only if the process includes "subtraction" of photons [6].

The enhancement, G, of optical processes due to aggregation of initially isolated particles into fractal cluster can be presented in general as

$$G \sim Q^m F(R_0^3|X|)\,, \tag{8}$$

where m is an integer and F is a function of dimensionless parameter $R_0^3|X|$. Using the model of randomly decimated (diluted) fractals [7] it was shown that F has power-law dependence[10]:

$$G \sim Q^m (R_0^3|X|)^{d_o+m} \tag{9}$$

for Rayleigh ($m=1$) and Raman ($m=3$) scattering. For the cluster–cluster aggregation the optical spectral dimension d_o is 0.3 [10]. In particular, formula (9) describes well the experimentally observed spectral dependence of surface-enhanced Raman scattering (SERS) on silver colloid aggregates [10]. The largest enhancement is expected for nonlinear light scattering like degenerate four-wave mixing (DFWM). In this case one obtains [10]

$$G \sim Q^6 (R_0^3|X|)^{2d_o+6}\,. \tag{10}$$

The experimentally observed enhancement of DFWM on silver fractal colloids [11] is in qualitative agreement with that predicted by (10).

To conclude, PSTM has been used successfully to observe, directly, the strong spatial localization of the resonant eigenmodes of fractals. This verifies the main concept predicted for the resonant optics of fractals [6–12] and explains the giant enhancement of optical processes in fractals.

We are grateful to A. Butenko and V. Gomer for the simulations presented in Fig. 1 and to J. Suh for assistance in preparation of samples.

References

[1] S. Alexander and R. Orbach, J. Phys. (Paris) Lett. 43 (1982) L1625;
R. Rammal and G. Toulouse, J. Phys. (Paris) Lett. 44 (1983) L13;
R. Bourbonnais, R. Maynard and A. Benoit, J. Phys. (Paris) 50 (1989) 3331.
[2] B. Sapoval, Th. Gobron and Margolina, Phys. Rev. Lett. 67 (1991) 2974.
[3] A. Bunde, H.E. Roman, S. Russ, A. Ahoroni and A.B. Harris, Phys. Rev. Lett. 69 (1992) 3189;
M. Schreiber and H. Grussbach, Phys. Rev. Lett. 67 (1991) 607.
[4] A. Petri and L. Pietronero, Phys. Rev. B 45 (1992) 12864;
F. Craciun, A. Bettucci, E. Molinari, A. Petri and A. Alippi, Phys. Rev. Lett. 68 (1992) 1555;
M. Montagna, O. Pilla, G. Viliani, V. Mazzacurati, G. Ruocco and G. Signorelli, Phys. Rev. Lett. 65 (1990) 1136.
[5] A. Bunde, ed., Fractals and Disorder (North-Holland, Amsterdam, 1992).
[6] V.M. Shalaev and M.I. Stockman, Zh. Eksp. Teor. Fiz. 92 (1987) 509 [Sov. Phys. JETP 65 (1987) 287]; Z. Phys. D 10 (1988) 71;
A.V. Butenko, V.M. Shalaev and M.I. Stockman, Zh. Eksp. Teor. Fiz. 94 (1988) 107 [Sov. Phys. JETP 67 (1988) 60]; Z. Phys. D 10 (1988) 81.
[7] V.A. Markel, L.S. Muratov and M.I. Stockman, Zh. Eksp. Teor. Fiz. 98 (1990) 819 [Sov. Phys. JETP 71 (1990) 455];
V.A. Markel, L.S. Muratov, M.I. Stockman and T.F. George, Phys. Rev. B 43 (1991) 8183.
[8] F. Claro and R. Fuchs, Phys. Rev. B 44 (1991) 4109;
K. Ghosh and R. Fuchs, Phys. Rev. B 44 (1991) 7330;

I.H. Zabel and D. Stroud, Phys. Rev. B 46 (1992) 8132.
[9] M.I. Stockman, T.F. George and V.M. Shalaev, Phys. Rev. B 44 (1991) 115;
V.M. Shalaev, R. Botet and A.V. Butenko, Phys. Rev. B 48 (1993) 6662.
[10] V.M. Shalaev, R. Botet and R. Jullien, Phys. Rev. B 44 (1991) 12216; 45 (1992) 7592(E);
M.I. Stockman, V.M. Shalaev, M. Moskovits, R. Botet and T.F. George, Phys. Rev. B 46 (1992) 2821;
V.M. Shalaev, M.I. Stockman and R. Botet, Physica A 185 (1992) 181.
[11] S.G. Rautian, V.P. Safonov, P.A. Chubakov, V.M. Shalaev and M.I. Stockman, Pis'ma Zh. Eksp. Teor. Fiz. 47 (1988) 243 [JETP Lett 47 (1988) 243];
A.V. Butenko, P.A. Chubakov, Yu.E. Danilova, S.V. Karpov, A.K. Propov, S.G. Rautian, V.P. Safonov, V.V. Slabko, V.M. Shalaev and M.I. Stockman, Z. Phys. D 17 (1990) 283.
[12] V.M. Shalaev, M. Moskovits, A.A. Golubentsev and S. John, Physica A 191 (1992) 352.
[13] R. Jullien and R. Botet, Aggregation and Fractal Aggregates (World Scientific, Singapore, 1987).
[14] E. Betzig and J.K. Trautman, Science 257 (1992) 189.
[15] D.P. Tsai, Z. Wang and M. Moskovits, SPIE Proc. 1855 (1993) 93.
[16] J.A. Creighton, Metal Colloids, in: Surface Enhanced Raman Scattering, R.K. Chang and T.E. Furtak, eds. (Plenum, New York, 1982).
[17] D.A. Weitz and M. Oliveria, Phys. Rev. Lett. 52 (1984) 1433.